Boundary-Layer Meteorology (2005) 116:253–276
DOI 10.1007/s10546-004-2817-1

MONIN–OBUKHOV SIMILARITY FUNCTIONS OF THE STRUCTURE PARAMETER OF TEMPERATURE AND TURBULENT KINETIC ENERGY DISSIPATION RATE IN THE STABLE BOUNDARY LAYER

O. K. HARTOGENSIS* and H. A. R. DE BRUIN
Meteorology and Air Quality Group, Wageningen University, Duivendaal 2, 6701 AP Wageningen, The Netherlands

(Received in final form 31 August 2004)

Abstract. The Monin–Obukhov similarity theory (MOST) functions f_ε and f_T, of the dissipation rate of turbulent kinetic energy (TKE), ε, and the structure parameter of temperature, ${C_T}^2$, were determined for the stable atmospheric surface layer using data gathered in the context of CASES-99. These data cover a relatively wide stability range, i.e. $\zeta = z/L$ of up to 10, where z is the height and L the Obukhov length. The best fits were given by $f_\varepsilon = 0.8 + 2.5\zeta$ and $f_T = 4.7[1 + 1.6(\zeta)^{2/3}]$, which differ somewhat from previously published functions. ε was obtained from spectra of the longitudinal wind velocity using a time series model (ARMA) method instead of the traditional Fourier transform. The neutral limit $f_\varepsilon = 0.8$ implies that there is an imbalance between TKE production and dissipation in the simplified TKE budget equation. Similarly, we found a production-dissipation imbalance for the temperature fluctuation budget equation. Correcting for the production-dissipation imbalance, the 'standard' MOST functions for dimensionless wind speed and temperature gradients (ϕ_m and ϕ_h) were determined from f_ε and f_T and compared with the ϕ_m and ϕ_h formulations of Businger and others. We found good agreement with the Beljaars and Holtslag [*J. Appl. Meteorol.* **30**, 327–341 (1991)] relations. Lastly, the flux and gradient Richardson numbers are discussed also in terms of f_ε and f_T.

Keywords: CASES99, Monin–Obukhov similarity scaling, Stable boundary layer, Structure parameter of temperature, TKE dissipation, Turbulent kinetic energy.

1. Introduction

Point source scintillometers have proven to be a good alternative method to obtain fluxes of heat and momentum in the stable boundary layer (SBL) (De Bruin et al., 2002; Hartogensis et al., 2002). The main advantage over the traditional eddy-covariance method is that turbulent fluxes can be obtained over short averaging intervals (~1 min and less) and close to the surface (less than 1 m), which are necessary conditions for measuring the often non-stationary and shallow SBL. Some key publications on scintillometry are Tatarskii (1961), Andreas (1990), Hill (1997) and De Bruin (2002).

The basic turbulent variables that are measured with scintillometers are the dissipation of turbulence kinetic energy (TKE), ε, and the structure

* E-mail: Oscar.Hartogensis@wur.nl

parameter of temperatures C_T^2. To determine the turbulent fluxes, use is made of the universal relationships between the dimensionless ε, and ${C_T}^2$ and the dimensionless height $\zeta = z/L$, where z denotes height and L the Obukhov length. These functions exist by virtue of the Monin–Obukhov similarity theory (MOST).

In spite of their practical relevance, little ε and ${C_T}^2$ data have been presented in the literature for $\zeta > 1$. It is the objective of this study to present experimental ε and ${C_T}^2$ and data for a stability range $0 < \zeta \lesssim 10$, from which we will derive new MOST functions. These data have been gathered in the context of the CASES-99 project (Poulos et al., 2002). We will compare our findings with previously reported MOST functions for ε and ${C_T}^2$; for instance Wyngaard (1973), Högström (1990), Thiermann and Grassl (1992), Frenzen and Vogel (2001), and Pahlow et al. (2001).

Assuming a production-dissipation balance of the TKE and temperature variance (T-variance) budget, the MOST functions for ε and ${C_T}^2$ are related to the MOST functions of the non-dimensional horizontal wind speed and potential temperature gradients, ϕ_m and ϕ_h respectively (Panofsky and Dutton, 1984), and through these also to the flux and gradient Richardson numbers. We will investigate these features and compare the thus derived ϕ_m and ϕ_h groups with the functions reported in the literature, e.g. the well-known ϕ_m and ϕ_h functions proposed by Businger et al. (1971).

2. Theory

According to MOST the following relations define the scaling relationships of ε and ${C_T}^2$ in the atmospheric surface layer:

$$\frac{\kappa z \varepsilon}{u_*^3} = f_\varepsilon(\zeta) \tag{1}$$

and

$$\frac{C_T^2 z^{\frac{2}{3}}}{\theta_*^2} = f_T(\zeta), \tag{2}$$

where z is the measurement height, κ the von Kármán constant (here taken as 0.4), θ_* the temperature scale, u_* the friction velocity, $\zeta \equiv z/L$ is a dimensionless height parameter with $L = Tu_*^2/\kappa g\theta_*$ is the Obukhov length and f_ε and f_T are universal MOST functions. In this study we will confine ourselves to stable conditions, i.e. $L > 0$.

A working hypothesis that is often used in TKE-budget analyses is that, close to the surface, the pressure and flux-divergence terms in the TKE equation are negligible (see e.g. Panofsky and Dutton, 1984). Consequently, the locally produced TKE by buoyancy and mechanical

turbulence is also locally dissipated, which often referred to as the 'local dissipation assumption'. The simplified TKE budget in non-dimensional form directly relates f_ε to the dimensionless gradient ϕ_m of the mean horizontal wind speed, $\bar{u}$:

$$f_\varepsilon = \phi_m - \zeta, \tag{3}$$

where ϕ_m, defined as $\phi_m(\zeta) = (\kappa z/u_*)\partial\bar{u}/\partial z$ represents mechanical TKE production, ζ represents buoyancy TKE production or destruction depending on the sign of ζ, and f_ε is the dimensionless dissipation rate.

Similar arguments for the T-variance budget equation lead to (Panofsky and Dutton, 1984):

$$f_T = \frac{3}{\kappa^{2/3}} \frac{\phi_h}{f_\varepsilon^{1/3}}, \tag{4}$$

where ϕ_h, the dimensionless gradient of mean potential temperature, $\bar{\theta}$, is defined as $\phi_h(\zeta) \equiv (\kappa z/\theta_*)\partial\bar{\theta}/\partial z$.

2.1. Similarity functions f_ε and f_T for ε and $C_T{}^2$

Hill (1997) gives an overview of several f_ε and f_T expressions for stable conditions that can be found in the literature.

In this study we will consider for f_ε:

$$f_\varepsilon(\zeta) = \left[1 + 2.3(\zeta)^{0.6}\right]^{\frac{3}{2}} \tag{5a}$$

proposed by Wyngaard and Cotė (1971) and adapted by Andreas (1989) to account for $\kappa = 0.4$ instead of 0.35,

$$f_\varepsilon(\zeta) = \left[1 + 4\zeta + 16(\zeta)^2\right]^{\frac{1}{2}} \tag{5b}$$

proposed by Thiermann and Grassl (1992),

$$f_\varepsilon(\zeta) = 0.85 + 4.26\zeta + 2.58(\zeta)^2 \tag{5c}$$

proposed by Frenzen and Vogel (2001) and

$$f_\varepsilon(\zeta) = c_{\varepsilon 1} + c_{\varepsilon 2}\zeta \tag{5d}$$

proposed by Wyngaard (1973). Several authors used Equation (5d) with different values for the constants $c_{\varepsilon 1}$ and $c_{\varepsilon 2}$; Wyngaard (1973) gave $c_{\varepsilon 1} = 1$ and $c_{\varepsilon 2} = 5$, Högström (1990) found $c_{\varepsilon 1} = 1.24$ and $c_{\varepsilon 2} = 4.7$, and, recently, Pahlow et al. (2001) obtained $c_{\varepsilon 1} = 0.61$ and $c_{\varepsilon 2} = 5$. The original form of Equation (5c) given by Frenzen and Vogel (2001) reads $f_\varepsilon = (0.85 + 0.6\zeta)(\phi_m - \zeta)$ with $\phi_m = 1 + 5.3\zeta$. In Equation (5c), we inserted their ϕ_m function in the f_ε expression. Frenzen and Vogel (2001) also gave a hyperbolic function of f_ε for the stable and unstable range.

They argued this function to be the best form since it is continuous for both the stable and unstable case and represented more closely the transition region between two regimes. Here we are interested in stable conditions and, therefore, will only consider their stable f_ε function.

Note that Hill (1997) cited Frenzen and Vogel (1992) wrongly in his literature overview of f_ε and f_T expressions. He gave $f_\varepsilon = 0.84 + 5\zeta$ for stable conditions after Frenzen and Vogel (1992), who indeed suggested $f_\varepsilon = 0.84$ for neutral conditions, but this result was obtained using only unstable data and no stable data were presented.

For $f_\varepsilon(0) \neq 1$, there is no balance between dissipation and production rates of TKE at neutral conditions. This follows directly from Equation (3), where it can be seen that $f_\varepsilon(0) = \phi_m(0)$, and $\phi_m(0)$ is 1 by the definition of the von Kármán constant. Frenzen and Vogel (1992, 2001) and Pahlow et al. (2001) found $f_\varepsilon(0) < 1$, whereas Högström (1990) found $f_\varepsilon(0) > 1$.

For f_T we will consider:

$$f_T(\zeta) = c_{T1}\left[1 + c_{T2}\zeta^{\frac{2}{3}}\right] \tag{6a}$$

after Wyngaard et al. (1971) with $c_{T1} = 4.9$ and $c_{T2} = 2.4$. We will use $c_{T2} = 2.2$ after Andreas (1989) to account for $\kappa = 0.4$ instead of $\kappa = 0.35$ used by Wyngaard. Thiermann and Grassl (1992) found

$$f_T(\zeta) = 6.34\left[1 + 7\zeta + 20\zeta^2\right]^{\frac{1}{3}}. \tag{6b}$$

2.2. Similarity functions ϕ_m and ϕ_h for $\delta u/\delta z$ and $\delta\theta/\delta z$

We will also investigate ϕ_m and ϕ_h expressions derived from f_ε and f_T, using Equations (3) and (4). As with f_ε and f_T, there is no unanimity in the literature on the formulations of ϕ_m and ϕ_h. In this study we will consider the Businger–Dyer relations (Businger et al., 1971; Dyer, 1974; Fleagle and Businger, 1980):

$$\phi_m(\zeta) = \phi_h(\zeta) = 1 + 5\zeta \tag{7a}$$

Recently, Andreas (2002) recommended the formulation of Holtslag and De Bruin (1988):

$$\phi_m(\zeta) = \phi_h(\zeta) = 1 + \zeta\left[a_1 + b_1\exp(-d\zeta) - b_1 d\left(\zeta - \frac{c}{d}\right)\exp(-d\zeta)\right] \tag{7b}$$

with $a_1 = 0.7$ and $b_1 = 0.75$, $c = 5$ and $d = 0.35$. Beljaars and Holtslag (1991) revised these expressions because Equation (7a) leads to flux Richardson numbers >1 for very stable conditions and arrived at:

$$\phi_m(\zeta) = 1 + \zeta\left[a + b\exp(-d\zeta) - bd\left(\zeta - \frac{c}{d}\right)\exp(-d\zeta)\right] \tag{7c1}$$

and

$$\phi_h(\zeta) = 1 + \zeta\left[a\left(1 + \frac{2}{3}a\zeta\right)^{\frac{1}{2}} + b\exp(-d\zeta) - bd\left(\zeta - \frac{c}{d}\right)\exp(-d\zeta)\right], \quad (7c2)$$

with $a = 1$, $b = 2/3$, $c = 5$ and $d = 0.35$

3. Experimental

3.1. Data description

We will use data gathered during CASES-99. The CASES-99 SBL experiment took place during October 1999 at a grassland site in Kansas, USA (Poulos et al., 2002). We operated a CSAT3 sonic anemometer from Campbell Scientific Inc., Logan, USA at 2.65 m. Raw 20 Hz data were stored on a laptop and processed afterwards with the latest version of the *EC-pack* flux-software package, developed by Wageningen University. The source code and documentation of the software can be found at http://www.met.wau.nl/projects/jep/index.html.

First, 5-min fluxes were calculated, which were subsequently averaged to 10-min values. The following corrections were performed in calculating the 5-min averaged fluxes:

- axis rotations were performed with the so-called planar fit routine after Wilczak et al. (2001). This routine fits the sonic's coordinate system to the time-averaged wind field that is assumed to be confined to a plane surface, nominally parallel to the ground. The planar fit rotations are based on a time interval that is much longer than the flux interval, in our case 24 h. We only used the planar fit rotations around the x- and y-axes. The rotation into the mean horizontal wind, around the z-axis, is done for every flux interval;
- sonic temperature was corrected for the influence of humidity and side-wind on the speed of sound measurement (Schotanus et al., 1983);
- fluxes were corrected for poor frequency response, i.e. flux loss due to sensor separation and sonic path averaging (Moore, 1986). For H this correction ranges between 15% for very stable conditions and less than 5% towards neutral conditions. For u_* the correction ranges between 7% for the very stable case and some 2% towards neutral conditions.

Vickers and Mahrt (2003) show that for stable conditions, more in particular for the CASES-99 dataset, the cospectral gap time scale of turbulence is surprisingly short, often only a few minutes. In this study we did not use flux-averaging periods that are adjusted to the turbulence encountered. Instead,

we chose to take a fixed flux averaging period of 5 min and assume that, on average, this time scale is such that we only include the turbulence contribution to the fluxes and exclude, larger scale, non-turbulence influences, such as gravity waves, drainage flows etc. The study of Vickers and Mahrt (2003) show that a 5-min averaging period gives less scatter than 30-min averaged fluxes in scaling relationships. Their gap time scale gives less scatter, however, and is regularly even shorter than 5 min.

We evaluated u_* including both the longitudinal and lateral components of the stress, i.e. $u_* = \left(\overline{u'w'}^2 + \overline{v'w'}^2\right)^{1/4}$.

3.2. Determining $C_T{}^2$ and ε from raw time series

$C_T{}^2$ is a scaling parameter of the temperature spectrum in the inertial range of turbulence and is defined as (e.g. Stull, 1988):

$$C_T^2 = \frac{D_T}{r^{2/3}} = \frac{\overline{[T(x) - T(x+r)]^2}}{r^{2/3}}, \tag{8}$$

where D_T denotes the structure function, $T(x)$ is the temperature at position x, $T(x+r)$ the temperature at position $x+r$, where r should lie within the inertial range of turbulent length scales. We calculated 10-min $C_T{}^2$ values from the 20 Hz sonic data using Taylor's frozen turbulence hypothesis to estimate a time lag that approximates best a space separation, r, of 1 m. We corrected for path averaging of the sonic temperature measurements after Hill (1991). Hartogensis et al. (2002) describe in more detail the $C_T{}^2$ calculation and correction procedure followed here.

Like $C_T{}^2$, ε is also a scaling parameter of spectra in the inertial range, in this case of TKE. For the longitudinal wind component, u, the inertial range of the spectrum, S_u, is described by

$$S_u(k) = \alpha \varepsilon^{2/3} k^{-5/3}, \tag{9}$$

where S_u is the spectral energy density, α is the Kolmogorov constant, and k is the spatial wavenumber expressed in cycles per unit length. We adopted $\alpha = 0.55$, which is mid-range of the values found in literature (e.g. Högström, 1996).

To obtain 10-min values of ε from 20 Hz sonic anemometer data the following procedure was followed:

First, the wind vector was rotated with the planar fit routine (Wilczak et al., 2001), and aligned to the mean wind direction, similarly as was done for the eddy-covariance fluxes described in Section 3.1.

Second, 10-min spectra of the longitudinal wind velocity, u, were calculated with the ARMASA toolbox, developed at the University of Delft, the Netherlands (Broersen, 2002; De Waele et al., 2002). ARMASA determines an optimal auto-regression (AR), moving-average (MA) time series model for

a given dataset from which $S_u(\kappa)$ can be determined directly. The principle advantages of spectra determined from ARMA models over conventional Fourier transforms are that the signal is not treated as a windowed periodogram where the first data point is treated as a neighbour of the last data point in the record, and no arbitrary smoothing of the spectrum is needed. ARMASA is written for MATLAB and is freely available at www.tn.tudelft.nl/mmr. We performed our analyses with ε determined with ARMASA and traditional Fourier transforms and found less scatter using ARMASA.

Third, we calculated ε using Equation (9) for all points of the spectrum.

Fourth, we performed a quality check on the spectrum and the calculated ε values to determine whether an inertial range was present in the spectrum. Moving point by point though the data, we determined the slope of the spectrum and the root mean square (rms) of ε for blocks of 25% of all the spectral points. An average ε was determined for all blocks for which the spectral slope deviated less than 20% of the theoretical $-5/3$ slope, and the rms of ε was less than 30% of its block-average value. When none of the blocks fulfilled these criteria, the ε value was rejected for that 10-min period.

Only stable conditions ($\zeta > 0$) between 1900 and 0700 are considered in this study. The data were selected on the following criteria: $\zeta > 0.0001$, $\overline{w'T'} < -0.0001$ K m s^{-1}, and $u_* > 0.01$ m s^{-1}. Data with one of these parameters falling below the given threshold values were excluded from the analysis.

4. Results and Discussion

Before presenting our results, we want to make a general comment on MOST scaling in the SBL. Under stable conditions the MOST assumption that $\frac{g}{T}\overline{w'T'}$, u_* and z are the relevant, independent scaling parameters might be questionable, because $\frac{g}{T}\overline{w'T'}$ and u_* are often interrelated, as is illustrated in Figure 1. Under stable conditions, the longwave radiation balance determines the 'strength' of the buoyancy parameter, $\frac{g}{T}\overline{w'T'}$. Under clear sky conditions the longwave radiation balance is dominated by the cooling rate at the surface, which, in turn, is strongly affected by wind speed. A high interrelationship between $\frac{g}{T}\overline{w'T'}$ and u_* exists therefore under clear sky conditions. Under cloudy conditions, the longwave radiation balance is also influenced by incoming radiation from clouds, and $\frac{g}{T}\overline{w'T'}$ and u_* will be more independent. Under these conditions, the stability is expected to be close to neutral.

4.1. Scaling functions for ε

Figure 2 shows our data of the ε dimensionless group, the f_ε scaling functions given by Equations (5a–d), and two f_ε curves that give a good fit to our data, namely

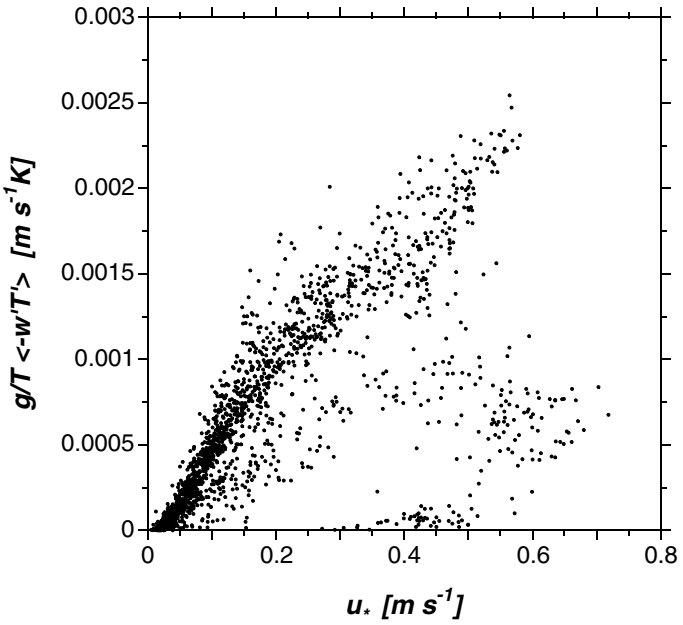

Figure 1. Scatter plot of 10-min eddy-covariance values of the buoyancy parameter, $\frac{g}{T}\overline{w'T'}$ against the friction velocity, u_*.

$$f_\varepsilon = 0.8 + 2.5\zeta, \tag{10a}$$

which is the Wyngaard (1973) form (Equation (5c)) with adjusted parameters $c_{\varepsilon 1}$ and $c_{\varepsilon 2}$, and a 'kink' function

$$f_\varepsilon = \begin{cases} 0.8 + 2\zeta & \text{for } \zeta < 0.1 \\ \frac{\sqrt{\zeta}}{\sqrt{0.1}} & \text{otherwise.} \end{cases} \tag{10b}$$

In the limit $\zeta \to \infty$ the formulations of Equations (10a) and (10b) differ. First, ε becomes independent of z in Equation (10a) (Pahlow et al., 2001), whereas in Equation (10b) ε remains a function of z. Second, as we will see later, the two formulations lead to different flux Richardson numbers.

For *near-neutral conditions*, we find that f_ε is less than 1, which implies there is an imbalance between TKE production and dissipation as was also reported by Frenzen and Vogel (1992, 2001), and Pahlow et al. (2001). Our f_ε neutral limit, $f_\varepsilon(0) \approx 0.8$ corresponds to the findings of Frenzen and Vogel (1992, 2001). Pahlow et al. (2001) found $f_\varepsilon(0) = 0.61$. Wyngaard et al. (1971) and Thiermann and Grassl (1992) imposed a production-dissipation balance in the TKE budget, their neutral limit of f_ε is therefore 1. Högström (1990) reported $f_\varepsilon(0)$ to be larger than 1, they found $f_\varepsilon(0) = 1.24$. When systematic

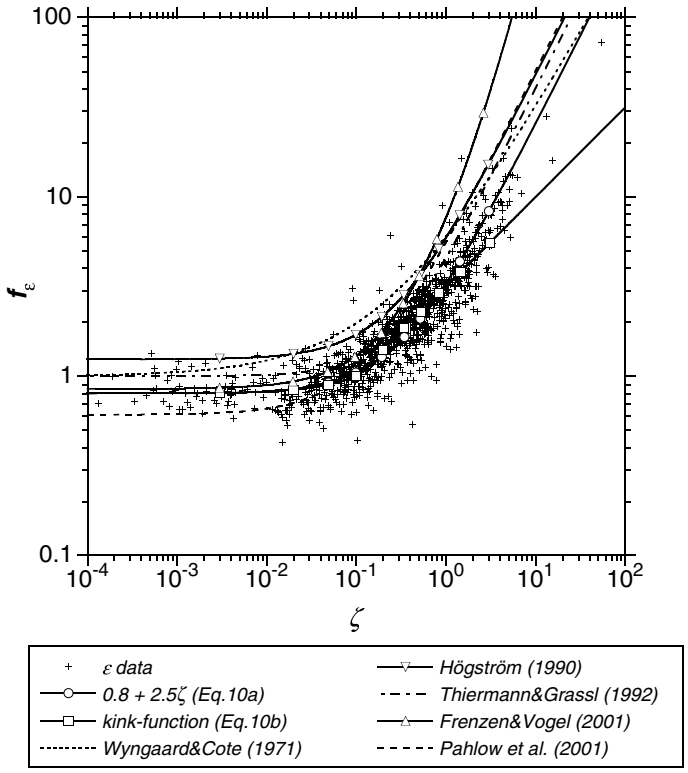

Figure 2. Dimensionless scaling group $f_\varepsilon = \kappa z \varepsilon / u_*^3$ of the TKE dissipation rate, ε, against the dimensionless stability parameter, ζ, for 10-min experimental values and relations found in literature.

measuring errors are assumed small, the imbalance between TKE production and dissipation found here implies that the pressure and flux-divergence terms in the TKE budget are not negligible. Högström (1996) suggests that the imbalance is most significant under near-neutral conditions where so-called inactive turbulence is important. Unfortunately, the pressure and flux-divergence terms of the TKE budget are very difficult to measure. Recently, Cuxart et al. (2002) presented data of the full TKE budget for one CASES-99 nights, and found that for that night the pressure and flux-divergence terms were indeed significant.

For *stable to very stable conditions*, we find that our f_ε values are lower than all other reported scaling functions.

There are several issues that play a role in the found differences between our scaling functions and the ones reported in literature so far.

First, the Kolmogorov constant, α, which we chose as $\alpha = 0.55$ in obtaining ε from the u spectra. Högström (1996) and Frenzen and Vogel (2001) give extensive discussions on this constant. The different values that

have been reported in the literature roughly vary between 0.5 and 0.6. The uncertainty in the Kolmogorov constant gives, relative to the $\alpha = 0.55$ we used, an approximate 10% uncertainty in ε. Note that the approach of Pahlow et al. (2001) in determining ε is parameter free but might be more sensitive to measuring errors since they use third order differences. The much lower $f_\varepsilon(0) = 0.61$ they found compared to our $f_\varepsilon(0) = 0.8$, cannot be explained by our choice of α. To obtain $f_\varepsilon(0) = 0.61$ from our data, we would have to use an α outside the range reported in the literature.

Second, since our aim is to find scaling relations for *turbulent* transport of momentum and heat, we tried to limit the influence of non-turbulent, non-local and non-stationary processes, such as drainage flows and gravity waves by choosing a short, 5-min time interval for our flux calculations and we ignored data points for which the u spectrum did not have a clear inertial sub-range (see Section 3.2). The study of Vickers and Mahrt (2003) shows that longer averaging periods, e.g. the standard 30-min period used by many investigators, give larger fluxes, but this is mainly attributed to non-turbulent contributions to the flux.

Third, our f_ε is based on a dataset that has a much larger ζ range than most other functions reported in the literature. This might explain that, apart from the neutral limit behaviour, f_ε from Thiermann and Grassl (1992), Frenzen and Vogel (2001) and Pahlow et al. (2001) are similar to our f_ε for $\zeta \lesssim 0.5$, but start to deviate for $\zeta \gtrsim 0.5$.

We evaluated u_* using the planar fit method to rotate the sonic into the mean wind field and including the lateral stress term $\overline{v'w'}$. Instigated by one of the referees we investigated whether another choice of evaluating u_* would make our results for f_ε more similar to what others have reported in the literature. Alternative rotation techniques we used were the double rotation method (which for each flux interval performs a rotation around the y- and z-axis of the sonic's coordinate system such that the average vertical and lateral wind components, $\bar{w}$ and $\bar{v}$, are zero) and the triple rotation method (which in addition to the double rotation method also performs a rotation around the x-axis such that the lateral stress, $\overline{v'w'}$, is zero). For the three rotation methods we evaluated u_* including and excluding the lateral stress. Note that for the triple rotation including or excluding the lateral stress makes no difference, since it is forced to zero. From this exercise the following can be concluded. The contribution of the lateral stress to the total u_* is only important when u_* is small (< 0.1) and ζ is large (> 0.8). Then, $\overline{v'w'}$ can contribute up to 80% of the total stress in some cases, whereas for larger u_* (> 0.1) and small ζ (< 0.8), the lateral stress contribution is less than 3%. Comparing u_* including the lateral stress for different rotation methods does not give large differences. The planar fit u_* gives marginally higher values, especially for low u_*, compared with the triple rotation method, and very similar values compared with the double rotation method. The differences

found for the various evaluations of u_* have very little effect on the found f_ε functions. The lower u_* values obtained when excluding the lateral stress extend the f_ε data points to higher ζ values, but they follow our f_ε-fit curve. This is due to the fact that both ε and ζ are scaled with u_*^{-3}, by which 'errors' in u_* appear to cancel when evaluating f_ε as function of ζ. This feature is further discussed in Section 4.3.

Next, we want to evaluate the ϕ_m scaling group from ε data using Equations (1) and (3). Equation (3) uses the local dissipation assumption, which, as discussed above, is violated for our dataset. We accounted for the TKE production-dissipation imbalance arbitrarily by dividing f_ε with its value in the neutral limit, i.e. we used

$$\phi_m = \frac{f_\varepsilon}{f_{\varepsilon\_cor}} + \zeta \tag{11}$$

with $f_{\varepsilon\_cor} = f_\varepsilon(0) = 0.8$ Note, that by scaling f_ε with its neutral value we ignore how the imbalance of TKE production and dissipation, i.e. the transport terms, may vary with stability. Figure 3 shows the comparison

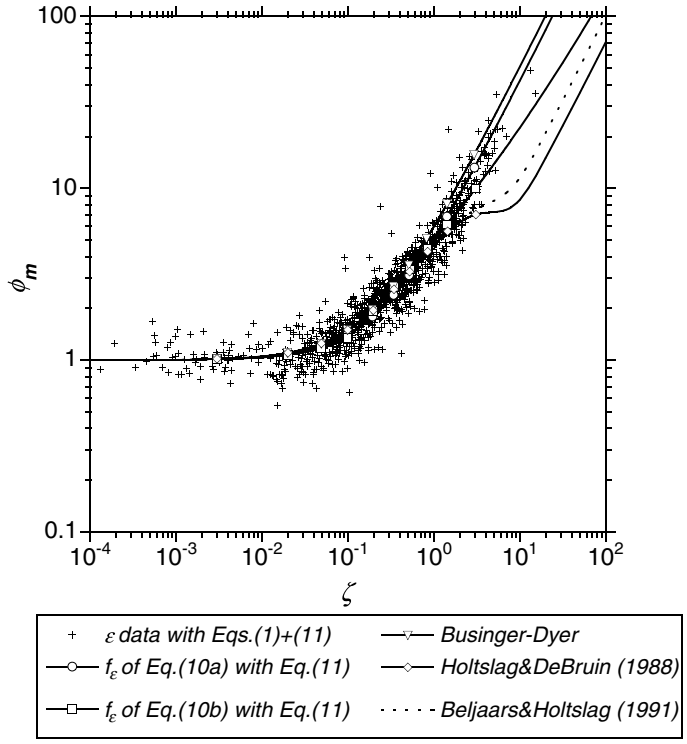

Figure 3. Dimensionless scaling group $\phi_m = (\kappa z/u_*)\partial\overline{u}/\partial z$ of the horizontal wind speed (u) gradient against the dimensionless stability parameter, ζ, for 10 min-experimental values based on $f_\varepsilon = \kappa z\varepsilon/u_*^{-3}$ using Equation (11), the f_ε relations of Equation (10) using Equation (11), and ϕ_m relations found in literature.

between the ϕ_m scaling group derived from ε data using Equations (1) and (11), the ϕ_m scaling functions derived from our f_ε expression of Equations (10a) and (10b) with Equation (11) and three ϕ_m functions found in the literature.

Now we will consider the ratio of the buoyancy destruction and the shear-production term, which is the definition of the flux Richardson number, R_f. R_f should approach a constant value smaller than 1 for very stable conditions where all turbulent motions are suppressed by buoyancy. Using the same imbalance correction described above for ϕ_m, we calculated R_f from our f_ε data and scaling functions using

$$R_f = \frac{\zeta}{\phi_m} = \frac{\zeta}{\frac{f_\varepsilon}{f_{\varepsilon\_cor}} + \zeta}. \tag{12}$$

In Figure 4, we plotted R_f for the same ε data, and f_ε and ϕ_m scaling functions as in Figure 3.

For $\zeta < 1$, Figures 3 and 4 show good agreement between ϕ_m and R_f from our adjusted f_ε functions and derived values from ε data, and the ϕ_m and

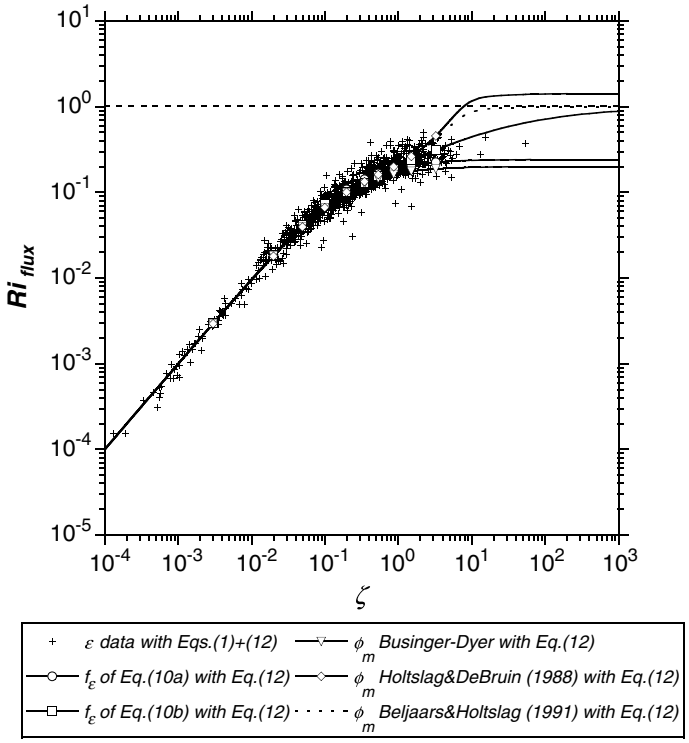

Figure 4. Flux Richardson number, Ri_{flux}, against the dimensionless stability parameter, ζ, for 10-min experimental values based on $f_\varepsilon = \kappa z \varepsilon / u_*^3$, the f_ε relations of Equation (10), and $\phi_m = (\kappa z / u_*) \partial \overline{u} / \partial z$ relations found in literature (see Equation (12)).

corresponding R_f functions found in the literature. In the neutral limit, for $\zeta < 0.1$, this agreement is forced by the correction we applied on our f_ε functions and data.

For $\zeta > 1$, the different ϕ_m curves and related R_f curves start to deviate. Figure 3 shows that, from the ϕ_m functions found in literature, the Businger–Dyer relation (Equation (7a)) agrees best with the derived values from our ε data. Furthermore, from the ϕ_m groups based on our f_ε functions, f_ε of Equation (10a) gives a slightly better fit than f_ε of Equation (10b). Figure 4, on the other hand, shows that in the stable limit, both the Businger–Dyer relation and the relation based on f_ε of Equation (10a) are well below 1. The R_f's from Beljaars and Holtslag (1991) ϕ_m function and our f_ε of Equation (10b) do approach the R_f limit of 1 for very stable conditions. The R_f of Holtslag and De Bruin (1988) goes to 1.4 in the very stable limit, which is a physically impossible value. Note that the data extend to $\zeta \approx 10$, where it does not yet reach the R_f limit of 1.

4.2. Scaling functions for $C_T{}^2$

Figure 5 shows our data of the $C_T{}^2$ dimensionless group, the f_T scaling functions given by Equations (6a) and (6b), and two f_T curves that give a good fit to our data, namely

$$f_T = 4.7\left[1 + 1.6\zeta^{\frac{2}{3}}\right], \tag{13a}$$

which is the function proposed by Wyngaard et al. (1971) given in Equation (6a) with different values for the constants c_{T1} and c_{T2}, and a 'kink' function

$$f_T = \begin{cases} 5.5 & \text{for } \zeta < 0.1 \\ 5.5\left(\frac{\zeta}{0.1}\right)^{\frac{2}{5}} & \text{otherwise.} \end{cases} \tag{13b}$$

It is seen that the scatter of the $f_T(\zeta)$ scaling group is much larger than the scatter of the $f_\varepsilon(\zeta)$ scaling group (Figure 2). In part this is explained by the difference in the propagation of errors in u_* and H for the $f_T - \zeta$ data pair compared to $f_T - \zeta$. This is further explained in Section 4.3. The uncertainty in f_T makes it difficult to discuss the differences between our f_T functions and the ones reported in the literature. As for f_ε, the chosen, short averaging period may affect f_T for $\zeta \gtrsim 0.1$. We did not investigate the effect of inclusion or exclusion of the lateral stress in u_* on Figure 5 as we did for Figure 2. If this plays a role it is for high ζ, where we already see a lot of scatter.

The f_T function of Thiermann and Grassl (1992) gives higher values than our observations. This suggests a production-dissipation imbalance of the T-variance budget in our data, since Thiermann and Grassl (1992) imposed a production-dissipation balanced budget.

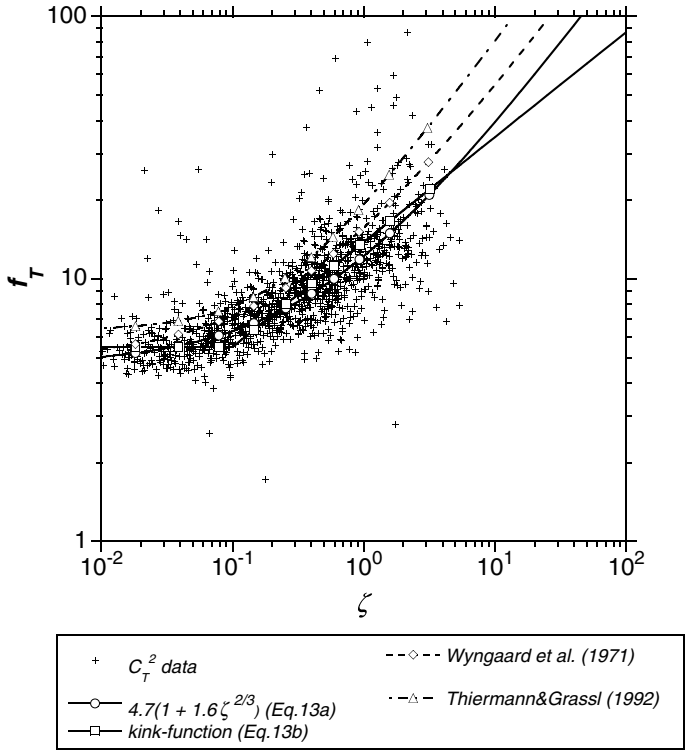

Figure 5. Dimensionless scaling group $f_T = C_T^2 z^{2/3}/\theta*^2$ of the structure parameter of temperature, C_T^2, against the dimensionless stability parameter, ζ, for 10-min experimental values and relations found in literature.

In evaluating the ϕ_h scaling group from $C_T{}^2$ and ε data using Equations (1), (2) and (4) we use the local dissipation assumption for the T-variance budget, which, as discussed above, is violated for our dataset. Equivalent to Equation (11) we therefore impose budget closure by dividing f_T with a constant value defined by its neutral limit value,

$$\phi_h = \frac{\kappa^{2/3}}{3}\left(\frac{f_\varepsilon}{f_{\varepsilon\_cor}}\right)^{\frac{1}{3}}\frac{f_T}{f_{T\_cor}}, \tag{14}$$

with $f_{T\_cor} = \frac{\kappa^{2/3}}{3} f_T(0)$ this gives $f_{T\_cor} = 0.85$ for f_T of Equation (13a) and $f_{T\_cor} = 0.99$ for f_T of Equation (13b). For the ϕ_h group from data we use $f_{T\_cor} = 0.9$.

Analogous to Figure 3, Figure 6 compares the ϕ_h scaling group derived from $C_T{}^2$ and ε data using Equations (1), (2) and (14), the ϕ_h scaling functions derived from our f_T expression of Equations (13a) and (13b) with Equation (14), and three ϕ_h functions found literature.

Next, using Equations (11) and (14), the gradient Richardson number can be expressed as

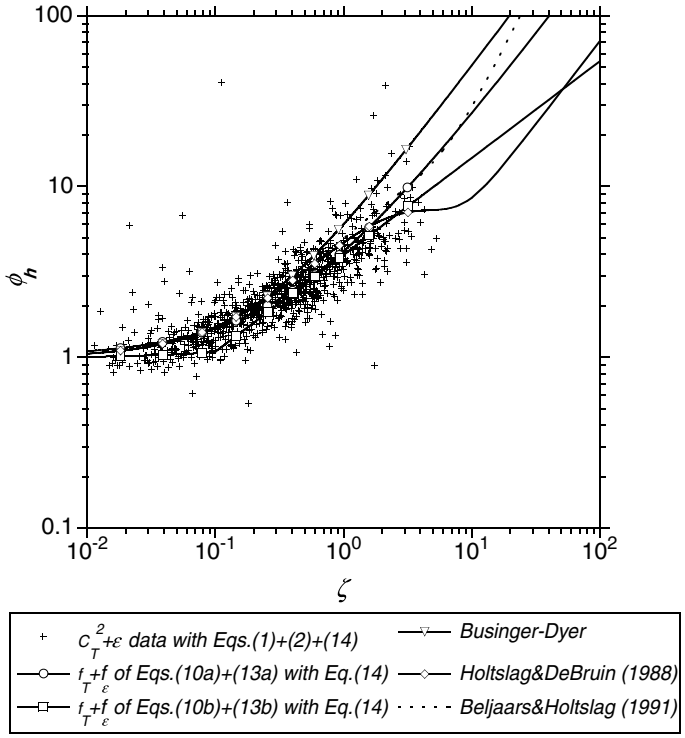

Figure 6. Dimensionless scaling group $\phi_h = (\kappa z/\theta_*)\partial\overline{\theta}/\partial z$ of the potential temperature (θ) gradient against the dimensionless stability parameter, ζ, for 10-min experimental values based on $f_\varepsilon = \kappa z\varepsilon/u_*^3$ and $f_T = C_T^2 z^{2/3}/\theta_*^2$ using Equation (14), the f_ε and f_T relations of Equations (10) and (13) using Equation (14), and ϕ_h relations found in literature.

$$Ri = \frac{\phi_h}{\phi_m^2}\zeta = \frac{\kappa^{2/3}}{3}\frac{\left(\dfrac{f_T}{f_{T\_cor}}\right)\left(\dfrac{f_\varepsilon}{f_{\varepsilon\_cor}}\right)^{1/3}}{\left(\dfrac{f_\varepsilon}{f_{\varepsilon\_cor}} + \zeta\right)^2}. \tag{15}$$

In Figure 7, we plotted *Ri* for the same C_T^2 and ε data, and f_ε, f_T and ϕ_m, ϕ_h scaling functions as in Figures 3 and 6.

For $\zeta < 1$, Figures 6 and 7 show good agreement between ϕ_h and *Ri* from our adjusted f_ε and f_T functions and derived vales from C_T^2 and ε data, and the ϕ_m, ϕ_h and corresponding *Ri* functions found in the literature. In the neutral limit, for $\zeta < 0.1$, this agreement is forced by the correction we applied on our f_ε and f_T functions and data.

For $\zeta > 1$, the different ϕ_h curves and related *Ri* curves start to deviate. Figure 6 shows that from the ϕ_h functions found in literature, the Beljaars–Holtslag relation (Equation (7c2)) agrees best with the values derived from our C_T^2 and ε data. Furthermore, from the ϕ_h groups based on our f_ε and f_T

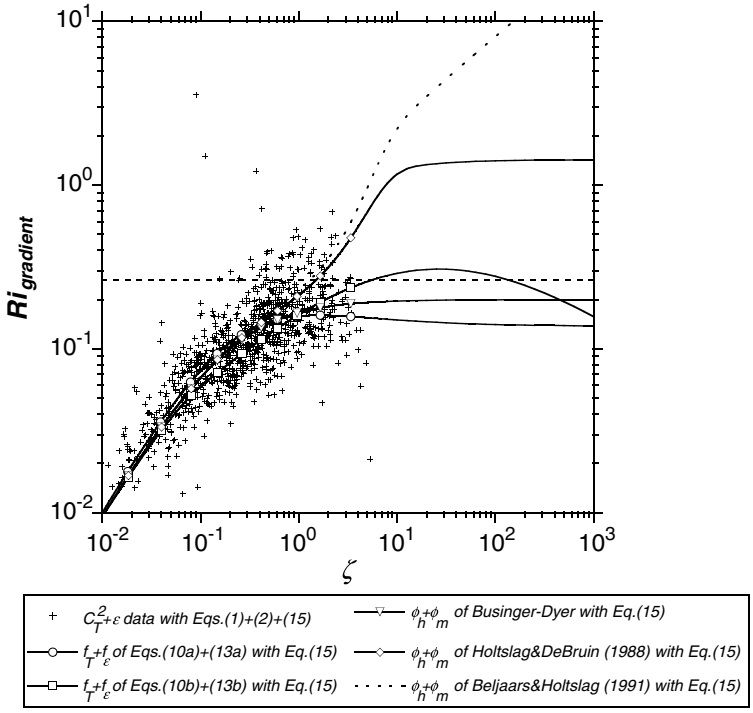

Figure 7. Gradient Richardson number, Ri_{gradient}, against the dimensionless stability parameter, ζ, for 10-min experimental values based on $f_\varepsilon = \kappa z\varepsilon/u_*^3$ and $f_T = C_T^2 z^{2/3}/\theta_*^2$, the f_ε and f_T relations of Equations (10) and (13), and $\phi_m = \kappa z/\theta_* \partial\bar{u}/\partial z$ and $\phi_h = \kappa z/u_* \partial\bar{\theta}/\partial z$ relations found in the literature (see Equation (15)).

functions, the f_ε–f_T of Equations (10a) and (13a) give a better fit than f_ε–f_T of Equations (10b) and (13b).

Recently, Pahlow et al. (2001) determined the dissipation rate of temperature fluctuations, ε_θ, which is related to $C_T{}^2$ through $C_T^2 = 2\varepsilon_\theta \varepsilon^{-1/3}$ (Panofsky and Dutton, 1984). They found that $\phi_{\varepsilon\theta}$, which is ε_θ made dimensionless with $\kappa z u_*/(\overline{w'T'})^2$, is about constant for $\zeta > 0.01$. In the case of a balanced temperature fluctuation budget, $\phi_{\varepsilon\theta}$ and ϕ_h are equal. Our ϕ_h data group based on f_ε–f_T formulations, which were forced to give TKE and temperature fluctuation budget closure in the neutral limit, is not constant for $\zeta > 0.01$.

Figure 7 shows that Ri seems to level off for $\zeta \to \infty$ to a limit just below the value often used for the critical Richardson number, $Ri_c = 0.25$. The value of Ri based on Beljaars and Holtslag (1991) and our f_ε–f_T functions of Equations (10b) and (13b) do not go to a stable limit value.

Our application of deriving ϕ_m and ϕ_h functions from single level ε and $C_T{}^2$ data might be a suitable alternative to ϕ_m and ϕ_h estimation from $\partial\bar{u}/\partial z$ and $\partial\bar{\theta}/\partial z$ for very stable conditions. Firstly, in these conditions gradients are difficult to determine accurately from discrete profile measurements.

Secondly, the SBL can be very shallow by which the constant flux approximation can be violated. The strong point of our approach is that we use single level data only. Obviously, the weak point is that we have to rely on the assumption that f_ε and f_T both scaled with their neutral value accounts for the non-closure of the TKE and T-variance budgets for the entire stability range. Our simple approach to correct for non-closure of the simplified TKE and T-variance budgets does yield good results; i.e. the derived ϕ_m and ϕ_h functions, and Richardson numbers evaluated in this way behave very similar to the functions found in the literature. Moreover, we were able to investigate ϕ_m and ϕ_h functions, and Richardson numbers for very stable conditions ($\zeta > 10$). In this study we used sonic measurements close to the surface, $z = 2.65$ m, and we already reach $\zeta \approx 10$. By doing the same analyses for sonics installed at higher levels, we should be able to extend the ζ range substantially.

4.3. Spurious correlations

Spurious correlations cannot be avoided when using MOST scaling (e.g. Hicks, 1981; De Bruin et al., 1993), since θ_* and u_* are present on both x- and y-axes of the scaling plots; on the y-axis to make variables dimensionless, and on the x-axis because θ_* and u_* define the Obukhov length. To test the scaling functions independently, without spurious correlation, we compared C_T^2 and ε, calculated indirectly from the eddy-covariance θ_* and u_* using the MOST relations given in Equations (10) and (13), with C_T^2 and ε determined from the raw data as described in Section 3.2. These two methods to obtain C_T^2 and ε are independent. The results depicted in Figure 8 show that C_T^2 and ε agree well, and the scatter is comparable to that of the scaling plots of Figures 2 and 5. This demonstrates that no significant, additional scatter is introduced due to the removal of the spurious correlation, and the effect of spurious correlation can therefore considered to be small.

One of the referees questioned whether the scatter seen in Figure 8a contains a hidden correlation with ζ. To demonstrate that this is not the case we plotted the percentage difference between the two independently derived ε values from Figure 8a as a function of ζ (not shown here). No systematic behaviour was found, which implies that the scatter seen in Figure 8a is indeed random. In addition, we carried out an exercise similar to that presented by Hicks (1981); i.e. we plotted the f_ε scaling group for measured u_* and ζ with random values of ε. If spurious correlation between f_ε and ζ dominates the function found then it is expected that the relation between the two is independent of ε. The measured ε values lie in a range between 10^{-3} and 10^{-1} m^2 s^{-3}. A random generator was used to produce the 10-exponent

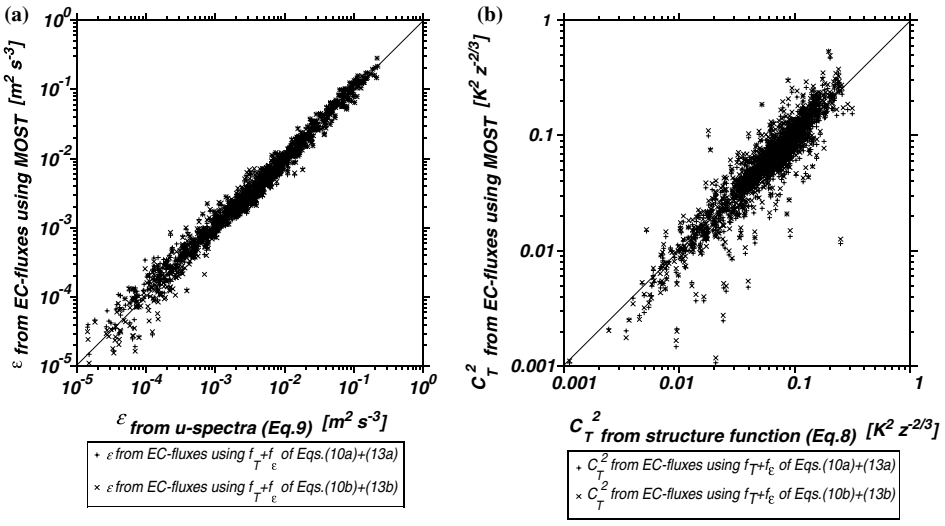

Figure 8. Comparison for the TKE dissipation rate, ε (a), and the structure parameter of temperature, $C_T{}^2$ (b) between values obtained from eddy-covariance fluxes using MOST and independent methods obtaining ε and $C_T{}^2$ from raw time series data.

values for ε between -1 and -3. In a plot similar to Figure 2 (not shown here), the f_ε data points with random ε do not follow the fitted f_ε function of Equation (10a), which demonstrates that the measured ε values determine the f_ε function found and not the shared ${u_*}^{-3}$ term on the x- and y-axes.

Although spurious correlation does not seem to determine the shape of the f_ε–ζ relation, it does affect the scatter found in the $f_\varepsilon-\zeta$ and $f_T-\zeta$ plots. Andreas and Hicks (2002) show how errors in u_* affect the scatter in ϕ_m and ϕ_h against ζ plots. Johansson et al. (2002) replied to this by stating that also the effect of errors in θ_* should be included. We performed such an analysis for $f_\varepsilon-\zeta$ and $f_T-\zeta$ plots, which shows that errors in u_* lead to a displaced $f_\varepsilon-\zeta$ pair that moves along the fitting curve, while a $f_T-\zeta$ pair moves normal to it. In other words, because of spurious correlation, errors in u_* result in enhanced scatter in f_T, and reduced scatter for f_ε. Errors in H only affect ζ in the $f_\varepsilon-\zeta$ plot, resulting in scatter along ζ axis. For f_T, errors in H result in a $f_T-\zeta$ pair that moves normal to the fitting curve, i.e. more scatter. In reality, the combined effect of errors in u_* and H on f_ε and f_T is more complex. Depending on the sign and size of the H and u_* errors, their individual effect on $f_\varepsilon-\zeta$ and $f_T-\zeta$ described above can either partly cancel out or enhance each other. If the errors in u_* and H are dependent these effects are systematic. In the absence of quantitative error estimates of u_* and H, we conclude that, based on the discussion here and the scatter found in Figures 2 and 5, the low scatter found for f_ε and high scatter found for f_T is due to spurious correlation.

4.4. Direct flux estimates from ε and C_T^2

We recall that our main motivation for this study was to find suitable MOST functions for C_T^2 and ε to obtain fluxes of heat and momentum using scintillometer measurements of C_T^2 and ε. Calculating these fluxes requires a numerical iteration of the f_ε and f_T functions. To be able to calculate the fluxes directly, without iteration, we introduce the dimensionless length scale, Z, derived from C_T^2 and ε

$$Z = \frac{g\kappa z}{T}\frac{T_C}{U_\varepsilon^2}, \tag{16}$$

in which $T_C = \sqrt{C_T^2 z^{2/3}}$ and $U_\varepsilon = \sqrt[3]{\kappa z \varepsilon}$ are a temperature and a wind speed scale.

Next, we searched for a relationship between Z and ζ and found the best fit for $\zeta = 0.55Z^{1.15}$. By substituting this empirical expression in the f_ε and f_T functions, one can directly calculate θ_* and u_*, and from these the kinematic sensible heat flux, $\overline{w'T'} = u_*\theta_*$.

Figure 9 compares u_* and $\overline{w'T'}$ calculated from ε and C_T^2 with this simplified approach against u_* and $\overline{w'T'}$ from ε and C_T^2 calculated by means of iteration. For both approaches the f_ε and f_T functions of Equations (10a) and (13a) are used. It is seen that the simplified approach can be used with little error.

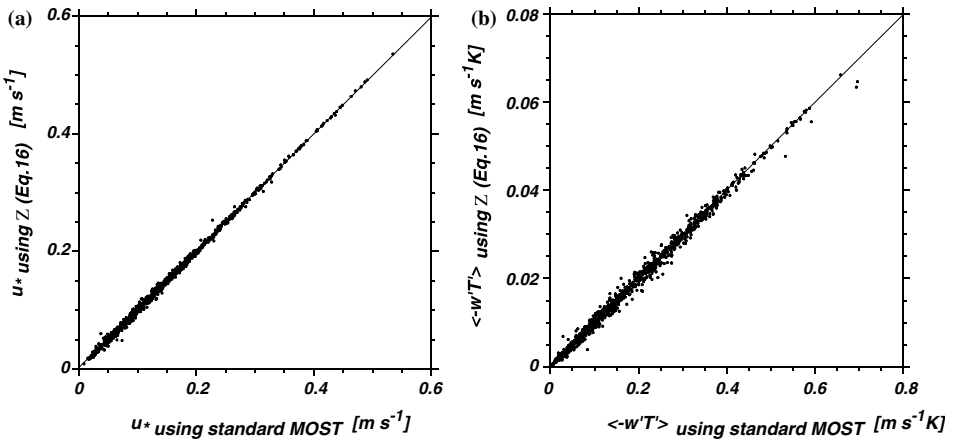

Figure 9. Comparison for the friction velocity, u_* (a) and kinematic heat flux, $-\overline{w'T'}$ (b) determined from the TKE dissipation rate, ε, and structure parameter of temperature, C_T^2, calculated directly with the alternative dimensionless height parameter, Z, of Equation (16), against the values calculated by means of numerical iteration of the MOST relationships given by Equations (10a) and (13a).

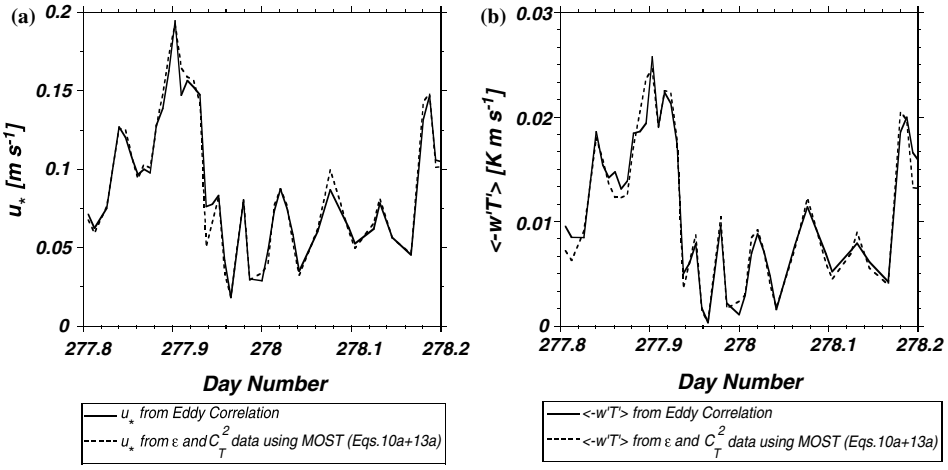

Figure 10. The friction velocity, u_* (a) and kinematic heat flux, $-\overline{w'T'}$ (b) determined from the TKE dissipation rate, ε, and structure parameter of temperature, $C_T{}^2$, using MOST and from eddy covariance as a function of time for the 'intermittent' night of 4 to 5 October.

4.5. Fluxes from ε and $C_T{}^2$ in intermittent turbulent conditions

A typical characteristic of turbulence in the SBL is that it is often intermittent, i.e. periods of laminar flow alternate with turbulent bursts. Hartogensis et al. (2002) showed an intermittent case during CASES-99, where a displaced-beam scintillometer was able to, at least qualitatively, measure the fluxes at a short enough time scale to resolve this phenomenon in great detail. In Figure 10 we compare, for that same night of 4 to 5 October, u_* and $\overline{w'T'}$ calculated from ε and $C_T{}^2$ using the f_ε and f_T functions of Equations (10a) and (13a) with the eddy-covariance u_* and $\overline{w'T'}$. It is seen that the ε and $C_T{}^2$ scaling performs well under these circumstances. De Bruin and Hartogensis (2005) show the same plot for the scaling of the standard deviation of temperature and longitudinal component of the wind speed, σ_T and σ_u, i.e. the variance method, which give less good results than the ε and $C_T{}^2$ scaling.

5. Conclusions

In this study we analysed the MOST scaling functions f_ε and f_T of the dissipation rate of TKE, ε, and the structure parameter of temperature, $C_T{}^2$, for the stable atmospheric surface layer using data we gathered in the context of CASES-99 (Poulos et al., 2002). These data cover a relatively wide stability range, i.e. ζ up to 10.

We found that $f_\varepsilon = 0.8 + 2.5\zeta$ and $f_T = 4.7[1 + 1.6\zeta^{2/3}]$ gave a good fit with our data. The alternative 'kink' functions, $f_\varepsilon = 0.8 + 2\zeta$ and $f_T = 5.5$ for

$\zeta < 0.1$, and $f_\varepsilon = \sqrt{\frac{\zeta}{0.1}}$ and $f_T = 5.5\left(\frac{\zeta}{0.1}\right)^{\frac{2}{5}}$ for $\zeta > 0.1$ gave a good fit also. Our results differ somewhat from those obtained by others such as Wyngaard and Coté (1971), Wyngaard (1973), Frenzen and Vogel (1992, 2001), Thiermann and Grassl (1992) and Pahlow et al. (2001). This might be related to a different data treatment – we used a short flux-averaging interval to exclude non-turbulent contributions to the flux (Vickers and Mahrt, 2003), and filtered our data based on inertial range behaviour in the longitudinal wind speed, and the fact that our ζ range was much larger than that used elsewhere.

Spurious correlation does not determine the shape of the f_ε function, but does affect the scatter seen in the $f_\varepsilon - \zeta$ and $f_T - \zeta$ plots. The propagation of errors in u_* and H leads to enhanced scatter in the $f_T - \zeta$ data pair and reduced scatter in the f_ε–ζ data pair because of spurious correlation.

In determining ε from the raw time series, we found that the ARMASA toolbox developed at the University of Delft (Boersen, 2002) is very suitable to obtain spectra from atmospheric turbulence time series. This approach has several advantages over the traditional Fourier transform method.

Since $f_\varepsilon(0)$ is found to be about 0.8 there is no balance between the production and dissipation terms in the TKE budget equations. Also, our results suggest a production-dissipation imbalance in the budget equation for temperature variance. This has been reported earlier by others.

Accounting for these imbalances using simple correction factors, we derived alternative expressions for the 'standard' MOST functions for dimensionless wind speed and temperature gradients, ϕ_m and ϕ_h from f_ε and f_T through the simplified budget equations for TKE and T variance. These compare well with the formulations proposed by Beljaars and Holtslag (1991). Note that our data cover a much wider stability range than most datasets using measured $\partial\overline{u}/\partial z$ and $\partial\overline{\theta}/\partial z$ to determine ϕ_m and ϕ_h. For instance, the Kansas dataset from which Businger et al. (1971) determined their ϕ_m and ϕ_h functions refer to $\zeta < 0.5$. Our results show that using ε and C_T^2 obtained from a single level sonic anemometer to derive ϕ_m and ϕ_h for very stable conditions is a good alternative, since, in that stability region, the measurement errors of gradients, especially $\partial\overline{u}/\partial z$, are large.

Our dataset did not allow us to study the very stable-limit value of the flux Richardson number, R_f, and the gradient Richardson number, Ri; i.e. a limit value was not reached for $\zeta \approx 10$. The different formulations for R_f, either derived from $\partial\overline{u}/\partial z$ and $\partial\overline{\theta}/\partial z$ or from ε data predict R_f limit values ranging from about 0.3 (Businger–Dyer) to 1 (Beljaars and Holtslag, 1991). Ri derived from f_ε and f_T through the budget equations for TKE and T variance appears to approach a limit just below the value often used for the critical Richardson number, $Ri_\mathrm{c} = 0.25$. This issue needs further research, i.e. the analyses need to be repeated for a wider ζ range.

For intermittent conditions, we found f_ε and f_T functions to perform very well in the estimation of u_* and $\overline{w'T'}$ from ε and $C_T{}^2$ measurements.

Acknowledgements

We thank Job Kramer and Bas Van de Wiel who helped with the field work during the CASES-99 experiment. The help of Steve Oncley and Gordon Maclean of NCAR during CASES-99 in offering technical support and use of the NCAR facilities on site is acknowledged. The first author received a NWO grant (nr. 810.33.005).

References

Andreas, E. L.: 1989, 'Two-wavelength Method of Measuring Path-averaged Turbulent Surface Heat Fluxes', *J. Atmos. Oceanic. Tech.* **6**, 280–292.

Andreas, E. L.: 1990, *Selected Papers on Turbulence in a Refractive Medium*, SPIE Milestone Series 25, SPIE – The International Society for Optical Engineering, Bellingham, 693 pp.

Andreas, E. L.: 2002, 'Parameterizing Scalar Transfer over Snow and Ice: A Review', *J. Hydrometeor.* **3**, 417–432.

Andreas, E. L. and Hicks, B. B.: 2002, 'Comments on "Critical Test of the Validity of Monin–Obukhov Similarity during Convective Conditions"' *J. Atmos. Sci.* **59**, 2605–2607.

Beljaars, A. C. M. and Holtslag, A. A. M.: 1991, 'Flux Parameterization over Land Surfaces for Atmospheric Models', *J. Appl. Meteorol.* **30**, 327–341.

Broersen, P. M. T.: 2002, 'Automatic Spectral Analysis with Time Series Models', *IEEE Trans. Instr. Measure.* **51**, 211–216.

Businger, J. A., Wyngaard, J. C., Izumi, Y., and Bradley, E. F.: 1971, 'Flux-Profile Relationships in the Atmospheric Surface Layer', *J. Atmos. Sci.* **28**, 181–189.

Cuxart J., Morales G., Terradellas E., and Yague C.: 2002, 'Study of Coherent Structures and Estimation of the Pressure Transport Terms for the Nocturnal Stable Boundary Layer', *Boundary-Layer Meteorol.* **105**, 305–328.

De Bruin, H. A. R., Kohsiek, W., and Van den Hurk, B. J. J. M., 1993, 'A Verification of Some Methods to Determine the Fluxes of Momentum, Sensible Heat and Water Vapour Using Standard Deviation and Structure Parameter of Scalar Meteorological Quantities', *Boundary-Layer Meteorol.* **63**, 231–257.

De Bruin, H. A. R., Van den Hurk, B. J. J. M., and Kohsiek, W.: 1995, 'The Scintillation Method Tested over a Dry Vineyard Area', *Boundary-Layer Meteorol.* **76**, 25–40.

De Bruin, H. A. R., Meijninger, W. M. L., Smedman, A. S., and Magnusson, M.: 2002, 'Displaced-Beam Small Aperture Scintillometer Test Part I: The WINTEX Data Set', *Boundary-Layer Meteorol.* **105**, 129–148.

De Bruin, H. A. R.: 2002, 'Introduction, Renaissance of Scintillometry', *Boundary-Layer Meteorol.* **105**, 1–4.

De Bruin, H. A. R. and Hartogensis, O. K.: 2005, 'Variance Method to Determine Fluxes of Momentum and Sensible Heat in the Stable Atmospheric Surface Layer', *Boundary-Layer Meteorol.* **6**, 385–392.

De Waele, S., Van Dijk, A., Broersen, P., and Duynkerke, P. G.: 2002, 'Estimation of the Integral Time Scale with Time Series Models', in *Proceedings 15th Symposium on Boundary*

Layers and Turbulence Diffusion, American Meteorological Society, Wageningen, Netherlands.

Dyer, A. J.: 1974, 'A Review of Flux-profile Relationships', *Boundary-Layer Meteorol.* **7**, 363–372.

Fleagle, R. G. and Businger, J. A.: 1980, *An Introduction to Atmospheric Physics*, 2nd edn., Academic Press, New York, 432 pp.

Frenzen, P. and Vogel, C. A.: 1992, 'The Turbulent Kinetic Energy Budget in the Atmospheric Surface Layer: A Review and Experimental Re Examination in the Field', *Boundary-Layer Meteorol.* **60**, 49–76.

Frenzen, P. and Vogel, C. A.: 2001, 'Further Studies of Atmospheric Turbulence in Layers near the Surface: Scaling the TKE Budget Above the Roughness Sublayer', *Boundary-Layer Meteorol.* **99**, 173–206.

Hartogensis, O. K., De Bruin, H. A. R., and Van De Wiel, B. J. H.: 2002, 'Displaced-Beam Small Aperture Scintillometer Test. Part II: Cases-99 Stable Boundary-Layer Experiment', *Boundary-Layer Meteorol.* **105**, 149–176.

Hicks, B. B.: 1981, 'An Examination of Turbulence Statistics in the Surface Boundary Layer', *Boundary-Layer Meteorol.* **21**, 389–402.

Hill, R. J.: 1991, 'Comparison of Experiment with a New Theory of the Turbulence Temperature Structure Function', *Phys. Fluids A* **3**, 1572–1576.

Hill, R. J.: 1997, 'Algorithms for Obtaining Atmospheric Surface-Layer Fluxes from Scintillation Measurements', *J. Atmos. Oceanic Tech.* **14**, 456–467.

Högström, U.: 1990, 'Analysis of Turbulence in the Surface Layer with a Modiefied Similarity Formulation for Near Neutral Conditions', *J. Atmos. Sci.* **47**, 1949–1972.

Högström, U.: 1996, 'Review of Some Characteristics of the Atmospheric Surface Layer', *Boundary-Layer Meteorol.* **78**, 215–246.

Holtslag, A. A. M. and De Bruin, H. A. R.: 1988, 'Applied Modeling of the Night-time Surface Energy Balance over Land', *J. Appl. Meteorol.* **27**, 689–704.

Johansson, C., Smedman, A-S., Högström, U., and Brasseur, J. G.: 2002, 'Reply to Comments on ''Critical Test of the Validity of Monin–Obukhov Similarity during Convective Conditions''', *J. Atmos. Sci.* **59**, 2608–2614.

Moore, C.: 1986, 'Frequency Response Corrections for Eddy Correlation Systems', *Boundary-Layer Meteorol.* **37**, 17–35.

Pahlow M., Parlange, M. B., and Porte-Agel, F.: 2001, 'On Monin–Obukhov Similarity in the Stable Atmospheric Boundary Layer', *Boundary-Layer Meteorol.* **99**, 225–248.

Panofsky, H. A., and Dutton, J. A.: 1984, *Atmospheric Turbulence: Models and Methods for Engineering Applications*, John Wiley & Sons, New York, 397 pp.

Poulos, G. S., Blumen, W., Fritts, D. C., Lundquist, J. K., Sun, J., Burns, S. P., Nappo, C., Banta, R., Newsom, R., Cuxart, J., Terradellas, E., Balsley, B., and Jensen, M.: 2002, 'CASES-99: A Comprehensive Investigation of the Stable Nocturnal Boundary Layer', *Bull. Amer. Meteorol. Soc.* **83**, 555–581.

Schotanus, P., Nieuwstadt, F., and De Bruin, H.: 1983, 'Temperature Measurement with a Sonic Anemometer and Its Application to Heat and Moisture Fluxes', *Boundary-Layer Meteorol.* **26**, 81–93.

Stull, R. B.: 1988, *An Introduction to Boundary Layer Meteorology*, Kluwer academic publishers, Dordrecht, 666 pp.

Tatarskii, V. I.: 1961, *Wave Propagation in a Turbulent Medium*, McGraw-Hill Book Company Inc., New York, 285 pp.

Thiermann, V. and Grassl, H.: 1992, 'The Measurement of Turbulent Surface-layer fluxes by Use of Bi-chromatic Scintillation', *Boundary-Layer Meteorol.* **58**, 367–389.

Vickers, D. and Mahrt, L.: 2003, 'The Cospectral Gap and Turbulent Flux Calculations', *J. Atmos. Oceanic Tech.* **20**, 660–672.

Wilczak, J. M., Oncley, S. P. and Stage S. A.: 2001, 'Sonic Anemometer Tilt Correction Algorithms', *Boundary-Layer Meteorol.* **99**, 127–150.

Wyngaard, J. C. and Cotë, O. R.: 1971, 'The Budgets of Turbulent Kinematic Energy and Temperature Variance in the Atmospheric Surface Layer', *J. Atmos. Sci.* **28**, 190–201.

Wyngaard, J. C., Izumi, Y., and Collins Jr., S. A.: 1971, 'Behavior of the Refractive Index Structure Parameter Near the Ground', *J. Opt. Soc. Amer.* **15**, 1177–1188.

Wyngaard, J. C.: 1973, 'On Surface Layer Turbulence', in D. A. Haugen (ed.), *Workshop on Micrometeorology*, Amer. Meteorol. Soc. pp. 101–149.